



# On optimal and varying decompositions for transradial contraction force prediction in upper-limb prosthesis

Ejay Nsugbe

Nsugbe Research Labs, Swindon, UK

## ARTICLE INFO

**Keywords:**  
Prosthesis Control  
Pattern Recognition  
LSDL  
Signal Processing  
Machine Learning

## ABSTRACT

The abilities to recognise an intended gesture alongside its associated contraction force are both useful features which could contribute towards the advancement of bionic upper-limb prosthesis. A substantial amount of related literature appears to address these problems separately instead of as part of a sequential control system. As part of an ongoing research on this topic, this work addresses the second portion of a multi-stage advanced prosthesis control system on the prediction of the contraction force used in producing a specific gesture motion. This problem was tackled using a novel decomposition method whose decomposition parameters could be varied based on a recognised gesture motion for an optimal decomposition of the sources signal, which is capable of maximising the prediction accuracy of the control system. The results showed a 10–20% increase in the classification accuracy using this method when compared with processing done with purely the raw acquired signal. Subsequent work would now involve the testing of this proposed control system on other categories of amputees such as transhumeral and shoulder disarticulation, in order to investigate its generalisation capability.

## 1. Introduction

The upper-limb of an individual is a meaningful portion of the human body, whose prime function is to support daily activities in addition to serving as a means towards navigating through the environment, thus the loss of an upper-limb has been seen to carry substantially life changing implications (Nsugbe et al., 2020a). These include the limitation of autonomy and independence, in addition to deeper problems such as distress due to concurring phantom sensations and the breaking of the individuals' biological motor control pathway (Nsugbe et al., 2020a). Some of the leading reasons for the loss of a portion of the upper-limb include trauma, conflict, and vascular diseases (Nsugbe et al., 2020a).

The bionic upper-limb prosthesis represents the closest engineered solution to a biological limb largely due to the functional capabilities, in addition to aiding the neurological rehabilitative purposes where the augmentation with a bionic upper-limb device contributes towards the forming of a 'cybernetic human motor control loop', which has been said to alleviate symptoms and distress of the amputated limb, therein serving as both a physical and neurological form of rehabilitation upon the loss of an upper-limb (Nsugbe, 2021c; ottobockus.com, n.d.). Due to varying extents of upper-limb loss, there also exist variations in the kinds of bionic upper-limb prosthesis which span transradial (below elbow

amputation), transhumeral (above elbow amputation), and shoulder disarticulation (Limbless Statistics, n.d.).

The deep literature on the research related to the design of the control interface for the various kinds of prosthesis reflects that there exists a unique kind of controller design challenge for each kind of prosthesis, where the majority of these control interfaces favour the pattern recognition control scheme for prosthesis due to its intuitiveness (Attenberger and Wojciechowski, 2017; Barry et al., 1986; Fougnier et al., 2012; Guo et al., 2014, 2015, 2017a, 2017b; Nsugbe, 2021a, 2021b). The success of the operability of this control scheme is centred on the successful recognition of the gesture intent motion, thus understandably, the majority of the emphasis in this area has been centred around effective means of solving the gesture recognition exercise in order to facilitate enhanced prosthesis control, where this exercise has been investigated using a mixture of healthy and amputee subjects (Attenberger and Wojciechowski, 2017; Barry et al., 1986; Fougnier et al., 2012; Guo et al., 2014, 2015, 2017a, 2017b; Nsugbe, 2021a, 2021b). To a lesser degree, researchers in the field have also investigated means towards predicting the contraction force of an identified gesture motion as part of the design of advanced prosthesis systems capable of varying their grip strengths (Doheny et al., 2008; Nazarpour et al., 2013).

Key work in this area was done by Al-Timemy et al. who, for a group

E-mail address: [ennsugbe@yahoo.com](mailto:ennsugbe@yahoo.com).

of transradial amputees, investigated the recognition of phantom motions in scenarios where the contraction force was seen to vary (Al-Timemy et al., 2015). The contributions made by Al-Timemy et al.'s work were centred around the recognition of gestures amidst varying forces, but were not extended towards a simultaneous prediction of contraction force alongside the gesture as a first step towards setting the velocity profile of the actuating motors in the prosthesis arm (Al-Timemy et al., 2015).

Thus, as part of an ongoing research study, this work utilises the acquired EMG data set acquired by Al-Timemy et al. (2015) towards the design of a multi-stage tiered pattern recognition controller that is capable of solving both the gesture recognition problem as well as the prediction of the associated contraction force. Prior work on this investigated the first part of the hypothesised control system which was focused on the gesture recognition problem using an amputee subject with a faint phantom motion EMG data set, where it was noted that the recognition accuracies of the developed model were enhanced greatly when the author-designed Linear Series Decomposition Learner (LSDL) was applied as a pre-processing mechanism to decompose the data and eliminate redundancy prior to the processing of the signal (Nsugbe, 2017, Unpublished results).

The decomposition approach for the LSDL worked with the assumption that a single set of decomposition parameters generalised across all six phantom gesture motions considered, and allowed for optimal signal decomposition (Nsugbe, 2017, Unpublished results). Although the obtained results showed this assumption to be valid, it is assumed that this assumption can be built on further by employing unique and customised LSDL decomposition parameters for each gesture set. At first, the limitation for the real-time implementation of this approach towards the signal decomposition is the need for an a-priori source capable of providing an initialisation which can cue in the unique parameters for the decomposition of a specific gesture motion. This assumed limitation can seemingly be overcome in this second aspect of the control system due to the gesture recognition problem being solved beforehand, and therein serving as form of a-priori information source that can provide an indication of the gesture intended by the amputee, and can thus cue in a set of LSDL decomposition parameters that are capable of an optimal decomposition of the source signal subsequent to signal processing, as means towards maximising the prediction accuracy. This approach was taken for the design of the second stage of the pattern recognition architecture and primed for the prediction of the contraction force intensity as part of the proposed multistage advanced control system.

The methodology adopted towards accomplishing this design was the variable gain controller framework, which relies on an external source as a means towards adaptively selecting the appropriate controller gain to adapt to an evolving/dynamically varying process, which in this study is a varying set of gestures (Analog.com, n.d.). An overarching diagram of the proposed multistage advanced control system can be seen in Fig. 1.

Specifically speaking, the contributions of this paper are as follows:

- The design of a 'variable gain' controller that is capable of adapting to varied gesture inputs, to subsequently yield an optimal signal decomposition which maximises the prediction accuracy
- The application of the designed prosthesis control system towards the prediction of the contraction force for an identified gesture motion whose performance is contrasted across three different classification models

## 2. Materials and methods

### 2.1. Data collection

The data used in this manuscript was collected by Al-Timemy et al. (2015) from an army based in Iraq where, as per previous work, the data utilised was from an amputee missing a portion of his left limb, as can be seen in Fig. 2. Further details regarding the amputee can be seen in Table 1 (Al-Timemy et al., 2015).

The collection of the data received ethical approval from the local governing authority and a written consent was provided prior to data collection (Al-Timemy et al., 2015). It can also be noted that skin preparation was done via cleansing with a combination of alcohol and a preparatory gel shortly before the placement of electrodes (Al-Timemy et al., 2015). The data was collected using electromyography (EMG) sensing using a 12-channel electrode, where the acquired data was sampled at 2000 Hz (Al-Timemy et al., 2015). The EMG signals represent a superposition and electrophysiological manifestation of action potentials from neuronal activities which are dependant on both the physiological and anatomical properties of an individual (E. Nsugbe, Samuel, Asogbon and Li, 2020). This can be mathematically modelled, using the principles of dipole theory, as a continuous stream of extracellular action potentials from a multi-source dipole, as described as follows (Nsugbe et al., 2020b):

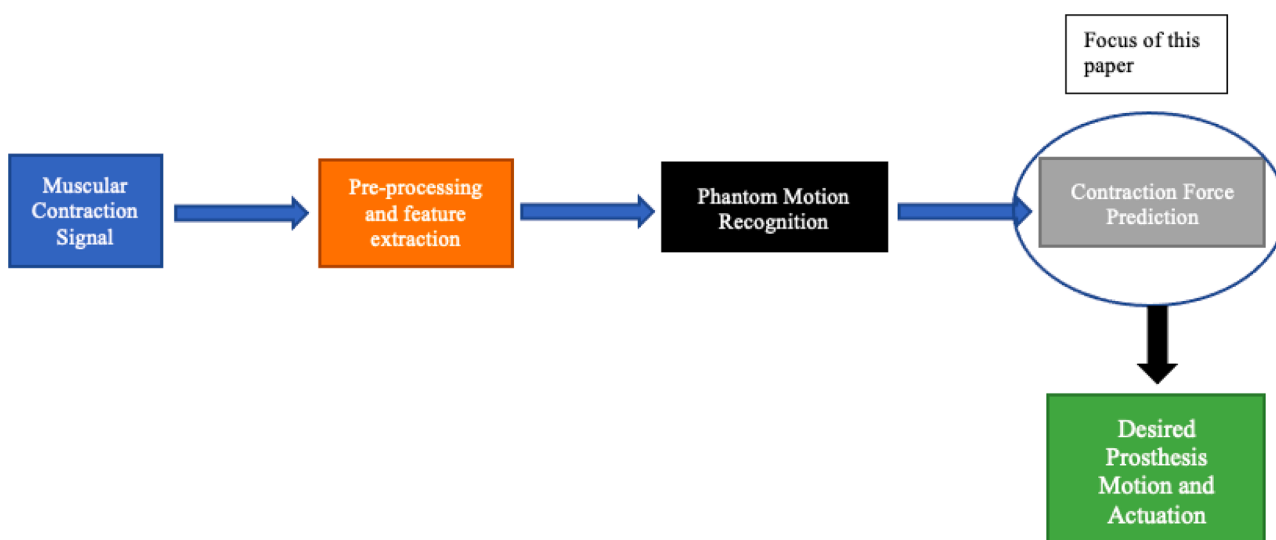


**Fig. 1.** Image of the proposed multistage prosthesis control architecture.



**Fig. 2.** Image of a transradial amputee missing a segment of his left upper-limb (Al-Timemy et al., 2015).

**Table 1**

Details on the amputee subject.

Age	Gender	Cause of Amputation	Stump Length	Stump Circumference	Time Since Amputation	Prosthetic Use
30	Male	Trauma	29.0 cm	23.5 cm	28 years	Cosmetic

$$\phi_e(t) = -\frac{a^2 \cdot \sigma_i}{4 \cdot \sigma_e} \int_{-\infty}^{+\infty} \frac{\partial IAP(x, t)}{\partial x} \cdot a_x^- \cdot \frac{\partial}{\partial x} \left( \frac{1}{r(x)} \right) dx \quad (1)$$

Where  $\phi_e$  is an extracellular potential which fluctuates with time,  $\sigma_e$  is a conductivity of the extracellular medium,  $\sigma_i$  is the intracellular conductivity,  $a$  is the fibre radius,  $t$  denotes time,  $r$  is the separation distance from the excitation source to the recording instrument,  $x$  is a point in space in the fibre element,  $a_x^-$  represents the span of the anatomical fibre, and  $\frac{\partial IAP}{\partial x}$  is a quantification of the dipole strength at a point within the fibre axis.

The gesture motions collected by Al-Timemy et al. (2015) spanned fine digit motions in addition to gripping motions, the majority of which can be said to be required in the daily activities of an individual. These gestures spanned the following: Spherical Grip (Gesture 1), Index Flexion (Gesture 2), Hook Grip (Gesture 3), Thumb Flexion (Gesture 4), Tripod Grip (Gesture 5), and Fine Pinch (Gesture 6); whilst a visual system indicated how much contraction force was being exerted (Al-Timemy et al., 2015). The contraction force variation aspect reflected a real-life case where the force exerted by an amputee had been seen to vary. For each gesture motion, three distinct contraction force levels were produced, namely, Low, Medium and High, where each contraction force was held in the range of 8–12 s. Details on the acquisition procedure for the various force levels can be seen in Al-Timemy et al. (2015), where it was described that the amputee expressed discomfort in producing the Low and High levels of contraction force due to a lack of use since the amputation. These levels of contraction forces caused pain and discomfort alongside a strenuous level of cognitive loading and sporadic bouts of tremor during the data collection process, which can be viewed as a source of uncertainty embedded within the collected data (Al-Timemy et al., 2015; Nsugbe, Unpublished results).

As with the prior related work, a trial spanning 10 s was used for each

level of contraction force alongside their respective gestures, and this was subsequently windowed via a series of disjointed windows to form repetitions sampled using a 250 ms windowing scheme.

## 2.2. Signal decomposition

The application of signal decompositions is based around an iterative separation and deconvolution of a signal in order to uncover embedded information and minimise the uncertainty within the signal (Daubechies, 1992). The applications of the concept span areas which gather both stationary and non-stationary trends and signals including physiological medicine, finance, and econometrics to name a few (Daubechies, 1992).

Amidst the various signal decomposition methods, the Linear Series Decomposition Learner (LSDL) has been seen to be powerful in terms of prediction capability and computationally efficient relative to its counterparts (Nsugbe and Sanusi, 2021; Nsugbe et al., 2016, 2018; Nsugbe et al., 2021). The technique is based around the use of an artificial intelligence (AI) driven agent which, given a set of initialisation parameters and a linear basis function, sequentially deconvolves a source signal whilst also being able to assess the information quality within each candidate decomposition region using a defined performance index (Nsugbe and Sanusi, 2021; Nsugbe et al., 2016, 2018; Nsugbe et al., 2021). The AI agent is structured on metaheuristic reasoning alongside a peak identification algorithm which, in tandem, serve as an automated set of rules to execute the desired computational action, alongside the filtration of the signal, to minimise redundancy and uncertainty for a candidate signal (Abdel-Basset et al., 2018).

In addition to its original inception case study, the LSDL has seen steady application across broad areas of clinical medicine involving physiological signals and spanning areas such as rehabilitation and pregnancy medicine (Nsugbe and Sanusi, 2021; Nsugbe et al., 2021). For each area, the LSDL has demonstrated a considerable improvement in

the recognition of physiological states when benchmarked against the state of the art, and therein showcased the ability of the technique to contribute towards an improvement in patient care strategies and, in certain cases, a greater potential to save lives (Nsugbe and Sanusi, 2021; Nsugbe et al., 2021).

From a technical perspective, given a sample signal  $|S_n|$ , an exhaustive list of the various step-by-step heuristics used during the decomposition process by the AI agent can be found in Nsugbe et al. (2021) and Nsugbe and Sanusi (2021), while this paper focuses on the description of the adaptation and utilisation of the LSDL's framework for the case study at hand. It can be noted that other decomposition methods exist in the literature such as the empirical mode decomposition (EMD), wavelet decomposition, and the decomposition packet in the statsmodel library, while the LSDL is a computationally effective approach that has seen prediction accuracy increase as a result of its application (Stallone et al., 2020; Statsmodels.org, n.d.; Talebi, 2022).

A tree-like hierarchical flow of the decomposition process can be seen in Fig. 3, where it is also shown how deconvolved decomposition regions are created during the implementation of the technique.

Mathematically speaking, the decomposition series can be expressed as follows:

$$|S_n| = \left( \int_0^T (T_{l_{upper1}})(|S_n|)dn + \int_0^T (T_{l_{upper2}})(|S_n|)dn \dots \int_0^T (T_{l_{upper_n}})(|S_n|)dn \right) + \left( \int_0^T (T_{l_{lower1}})(|S_n|)dn + \int_0^T (T_{l_{lower2}})(|S_n|)dn \dots \int_0^T (T_{l_{lower_n}})(|S_n|)dn \right) \quad (2)$$

$$|S_n| = \int_0^T \left( Upr_n(|S_n|) + \int_0^T Lwr_n(|S_n|) \right) dn \quad (3)$$

For the computation of the optimal decomposition region, the low and medium contraction forces were utilised as these represent faint contraction signals whose motions can be thought to be challenging to predict. This approach was carried for all the contraction forces across all six gesture sets, across four defined iterations for both the upper and lower threshold regions to yield a total of 48 simulations, and to obtain the various values presented in Table 2.

A summary table showing the LSDL optimal decomposition regions for the contraction force for all six gestures can be seen in Table 3.

From Table 3 it can be noted that the optimal threshold region varies based on the gesture at hand, thus it can be said that the prediction accuracy of a contraction force can be maximised if the threshold is varied and based on a recognised gesture within the prosthesis control system. In the previous related work on the gesture recognition aspect of the control system, a generalised threshold approach had to be adopted in the recognition of gestures as this was the first stage of the system without the presence of any a-priori or reference input regarding the intended gesture motion. This section of the control system hinges upon the solving of the gesture recognition problem, which can therein serve as a cue and reference input that can be used in the selection of the appropriate threshold model to decompose the input signal subsequent to the prediction of the contraction force. A mentioned, this methodology closely resembles the concept of a variable gain control system with applications in optics and audio mixing, where the gains of an electronic device are varied to optimise performance based on an optical measurement from a light emitting diode or a reference current value.

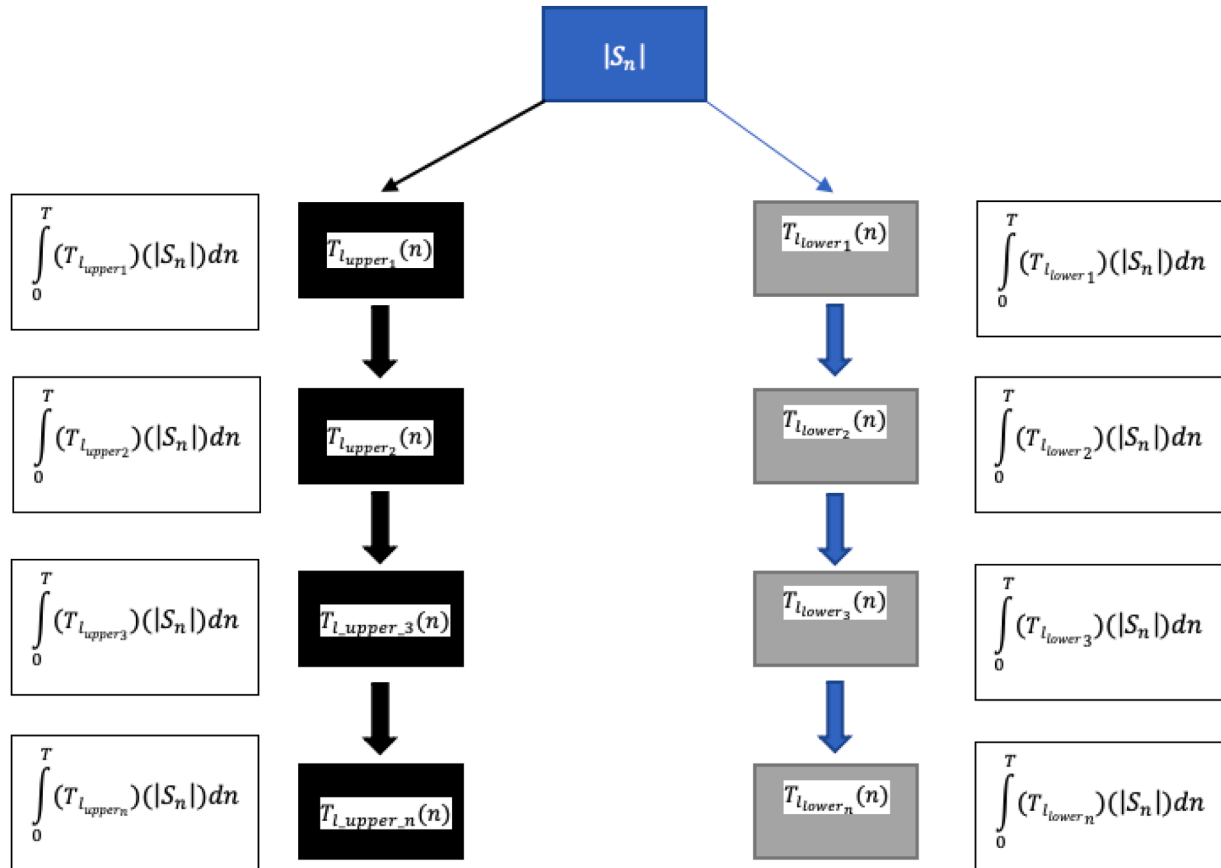


Fig. 3. Decomposition tree representation for the LSDL (where  $T$  indicates the length of the candidate signal) (Nsugbe et al., ).

**Table 2**  
Performance Index Results for the LSDL decomposition of the various gestures.

Gesture 1	Iteration	1	2	3	4
Upper threshold region		2.0000	n/a	n/a	n/a
Lower threshold region		2.0731	2.0730	2.0531	2.0415
Gesture 2					
Iteration	1	2	3	4	
Upper threshold region	n/a	n/a	n/a	n/a	
Lower threshold region	2.0403	2.0020	2.0082	2.0320	
Gesture 3					
Iteration	1	2	3	4	
Upper threshold region	2.0309	n/a	n/a	n/a	
Lower threshold region	2.0164	2.0303	2.0332	2.0442	
Gesture 4					
Iteration	1	2	3	4	
Upper threshold region	n/a	n/a	n/a	n/a	
Lower threshold region	2.0014	2.0066	2.0240	2.0255	
Gesture 5					
Iteration	1	2	3	4	
Upper threshold region	2.0210	n/a	n/a	n/a	
Lower threshold region	2.1226	2.1388	2.1018	2.1368	
Gesture 6					
Iteration	1	2	3	4	
Upper threshold region	n/a	n/a	n/a	n/a	
Lower threshold region	2.0388	2.0573	2.0442	2.0457	

n/a indicates a lack of availability of samples to compute a performance index.

### 2.3. Feature extraction

Various forms of feature engineering methods exist which allow for a streamlined approach towards selecting the optimal subsets of features, including the catch22 and FLOps algorithms (Lubba et al., 2019; Patel et al., 2020). As this area of signal processing has been addressed substantially over the years, it is known which sets of features are optimal for these applications and thus would be applied in this study, negating the need for the application of any form of feature engineering methods (CompEngine, n.d.; Lubba et al., 2019; Patel et al., 2020).

The same feature group used in the gesture recognition aspect was used in this study and includes a set of computationally efficient features, as follows: mean absolute value (MAV), fourth order autoregression (AR), simple square integral (SSI), enhanced mean absolute value (EMAV), log detector (LD), Wilson amplitude (WAMP), variance (VAR), root mean square (RMS), kurtosis (Kurt), and maximum ceps-trum coefficient (Ceps) (Too et al., 2019).

### 2.4. Classifiers

Similar to the feature sets, the following classifiers were adopted from the previous exercise on gesture recognition: the white box-based non-parametric decision tree (DT) model; and the support vector machine (SVM) kernel-based model, where both the linear (L-SVM) and quadratic based (Q-SVM) variants of the SVM were utilised in this study (Nsugbe et al., 2021; Sharma and Kumar, 2016). The L-SVM uses a linear decision boundary towards separation of the various data classes, while the Q-SVM—which has a more complex architecture—utilises a non-linear decision boundary towards the separation of data classes where, explicitly in this case, a quadratic function is used for the class boundaries.

Although it can be acknowledged that a range of classification models exist in the literature, this set of models was chosen for this work due to being computationally efficient, which is crucial for real-time

application purposes in this area of research (auto-sklearn, n.d.; Brownlee, 2020; scikit-learn, n.d.). The MATLAB 2020a Machine Learning Toolbox was used for all model builds. As part of this process, optimal hyperparameters were tuned with respect to a unique optimisation cost function for each model, and subsequently validated using the hold-out method, where 80% of the data was used in the training process of the classifiers and the remaining 20% used to test the performance of the trained classifier.

## 3. Results

The results from the classification exercises can be seen in Table 4 where, for the majority of the gestures, the LSDL produced the optimal accuracy and also boasted a 10–20% increase in the mean classification accuracy across all gestures, therein showcasing the power of the LSDL in enhancing the prediction power through its decomposition prowess. The results are also in line with what was obtained in the prior related work on gesture recognition, where the LSDL produced the best performance in gesture recognition when compared with the raw signal.

Given that three classifiers were trained in this study, it is possible to maximise the overall prediction performance by selecting the classification model which produces the best classification performance for each gesture set. It can be seen in Table 5 that there is a variation amongst the list of optimal classifiers for the six gestures, therein showing the variation in the overall behaviour of these kinds of electrophysiological signals acquired from amputees.

The computation times for each of the various classifiers can be seen in Table 6, and were produced using five repetitions for each classifier. It can be seen that the DT classifier continues to provide the most optimal computation time for the classification problem, although the different variants of the SVM are also within range. It can also be noted that the selection times for the various classifiers are reasonably lower than that of the prior gesture recognition problem due to the problem of the contraction force prediction comprising of three classes, as opposed to the gesture recognition problem which is a broader problem consisting of six classes.

The principal component analysis (PCA) plot allows for a lower dimensional visualization of the degree of separation between the various data classes considered as part of the recognition and classification problem. From Fig. 4 the top plot shows a visualization and therein the degrees of separability of the various classes plotted for Gesture 2, which can be seen to contain a substantial level of overlap amongst the various classes and provides a degree of qualitative explanation as to the relatively low classification accuracy recorded in Table 4. The bottom plot of Fig. 4 shows the visualization for the signals that were pre-processed by the LSDL, which can be seen to show a much greater leave of separation between the various classes and again provides qualitative evidence to show the impact and benefits of the LSDL decomposition method, while also providing further signs to explain the relatively higher classification accuracy recorded as part of Table 4. An image of the advanced pattern recognition control system can be seen in Fig. 5.

## 4. Conclusion

The loss of a portion of the upper-limb can severely impair the level of independence of an individual in addition to the quality of life which they are afforded. The bionic upper-limb prosthesis replicates as closely as possible to a functional upper-limb due to the functionality which it

**Table 3**  
Summary table showing the various optimal decompositions for each gesture.

Gesture number	1	2	3	4	5	6
Threshold region	Lower region iteration 1	Lower region iteration 1	Lower region iteration 4	Lower region iteration 4	Lower region iteration 2	Lower region iteration 2

**Table 4**

Classification comparison of results of the raw data and the LSDL decomposition.

	Raw-DTClassification Accuracy (%)	LSDL-DTClassification Accuracy (%)	Raw L-SVMClassification Accuracy (%)	LSDL L-SVMClassification Accuracy (%)	Raw Q-SVMClassification Accuracy (%)	LSDL Q-SVMClassification Accuracy (%)
<b>Gesture 1</b>	74.0	59.3	68.9	65.6	<b>76.9</b>	63.7
<b>Gesture 2</b>	64.5	<b>80.6</b>	60.1	<b>80.6</b>	68.9	<b>80.6</b>
<b>Gesture 3</b>	57.9	84.2	47.3	86.4	58.6	<b>88.6</b>
<b>Gesture 4</b>	48.0	<b>75.5</b>	57.9	49.8	60.1	51.3
<b>Gesture 5</b>	68.9	90.1	61.9	95.6	69.6	<b>96.0</b>
<b>Gesture 6</b>	61.2	81.7	44.3	88.3	60.1	<b>90.8</b>
<b>Mean</b>	62.40 ± 8.27	78.60 ± 9.65	56.70 ± 8.48	77.70 ± 15.50	65.70 ± 6.63	78.50 ± 15.93

**Table 5**

List of optimal classifiers alongside the classification accuracies.

	Optimal Classifier	Classification Accuracy (%)
<b>Gesture 1</b>	L-SVM	76.9
<b>Gesture 2</b>	DT/L-SVM/Q-SVM	80.6
<b>Gesture 3</b>	Q-SVM	88.6
<b>Gesture 4</b>	DT	75.5
<b>Gesture 5</b>	Q-SVM	96.0
<b>Gesture 6</b>	Q-SVM	90.8
<b>Mean</b>		84.7 ± 7.6

**Table 6**

Table showing selection time for the three classification models.

Selection Time-DT(for the prediction of a single instance) (ms)	Selection Time-l-SVM (for the prediction of a single instance) (ms)	Selection Time-Q-SVM (for the prediction of a single instance) (ms)
15.60 ± 10.64	22.70 ± 4.31*	22.36 ± 3.66*

\* Although the selection time for both the l-SVM and Q-SVM are of somewhat similar timeframes, it can be noted that the training time of the Q-SVM is considerably longer than that of the l-SVM (although not displayed here).

affords its users. The functionality of the bionic upper-limb prosthesis hinges upon the control interface responsible for converting an acquired neuromuscular signal into an effective machinery actuation prompt which is capable of performing the trained and intended gesture motion. The bulk of the studies in the literature are primarily centred around the solving of the gesture recognition system as part of the pattern recognition controller, with only a small number of authors considering the prediction of the associated force as part of a more complex prosthesis control interface.

This paper presents the progress made in an ongoing study poised around the design of a tiered pattern recognition control system which is capable of first recognising the intended gesture motion with signals obtained from a set of EMG sensors, then subsequently predicting the associated contraction force, as part of an advanced prosthesis control system. As part of the research, this paper builds on the results from the prior study on the recognition of an intended gesture motion using a generalised LSDL algorithm, which contributed towards an increase in the recognition accuracies of gesture motions.

The focus and contribution of this paper has been based around the design of the second portion of the proposed advanced control system architecture for the subsequent prediction of the associated contraction force accompanying an intended gesture motion. The control architecture for this aspect of the advanced control system is formulated using a variable gain control architecture which leverages the solution of the a-priori solved gesture recognition problem, and applies this as a reference towards tuning into the various LSDL parameters which are customised

towards an optimal decomposition of each specific gesture motion. The overall results showed a 10–20% increase depending on the classification models used, which was further increased and optimised through a classifier selection process, as shown in Table 5. This architecture – alongside the gesture recognition portion of the proposed system – is an advanced pattern recognition-based control system which is capable of solving the recognition problem alongside subsequently predicting the necessary contraction force for performing the gesture, and forms a more realistic bionic interface that can allow for further ‘humanisation’ of the bionic limb. The varied grip strength of the prosthesis limb allows for the amputee to interact with various kinds of objects in their daily life (from fragile eggs to heavy text books, for example) and adds a layer of autonomy to the amputee’s life, where they are no longer constrained in their interactions with objects based on a default grip strength. Benchmarking this against prior key work in the literature by Al-Timemy et al., this work presents an advancement on the existing work as the prior literature only considered an aspect and component of the overall problem presented in this paper, whereas the work presented in this manuscript showcases an advanced tiered prosthesis control system where phantom motions are recognised a-priori and subsequently followed by the prediction of the contraction force for each specific motion (Al-Timemy et al., 2015). And therein presents a substantial advancement when compared with the existing literature.

This pilot work has been done with a transradial subject’s dataset and with EMG sensing; subsequent work could involve testing this designed advanced prosthesis control system on data from transhumeral and shoulder disarticulation subjects who have been previously seen to produce neuromuscular signatures with greater stochasticity as well as the trial and testing of other classification model tuning methods such as the AutoSKLearn (Nsugbe and Al-Timemy, 2021; Nsugbe et al., 2021). Also, the use of probabilistic modelling can be included in both aspects of the prosthesis control system in order to serve as an algorithmic function to minimise mis-recognition of gestures using a probabilistic thresholding method where only samples with a high level of certainty are pruned out and are subsequently proceeded towards the classification stage of the overall system (Cao et al., 2015).

#### Author statement

Ejay Nsugbe-Result analysis and paper draft.

#### Declaration of Competing Interest

The author declares that there is no conflict of interest regarding the publication of this article.

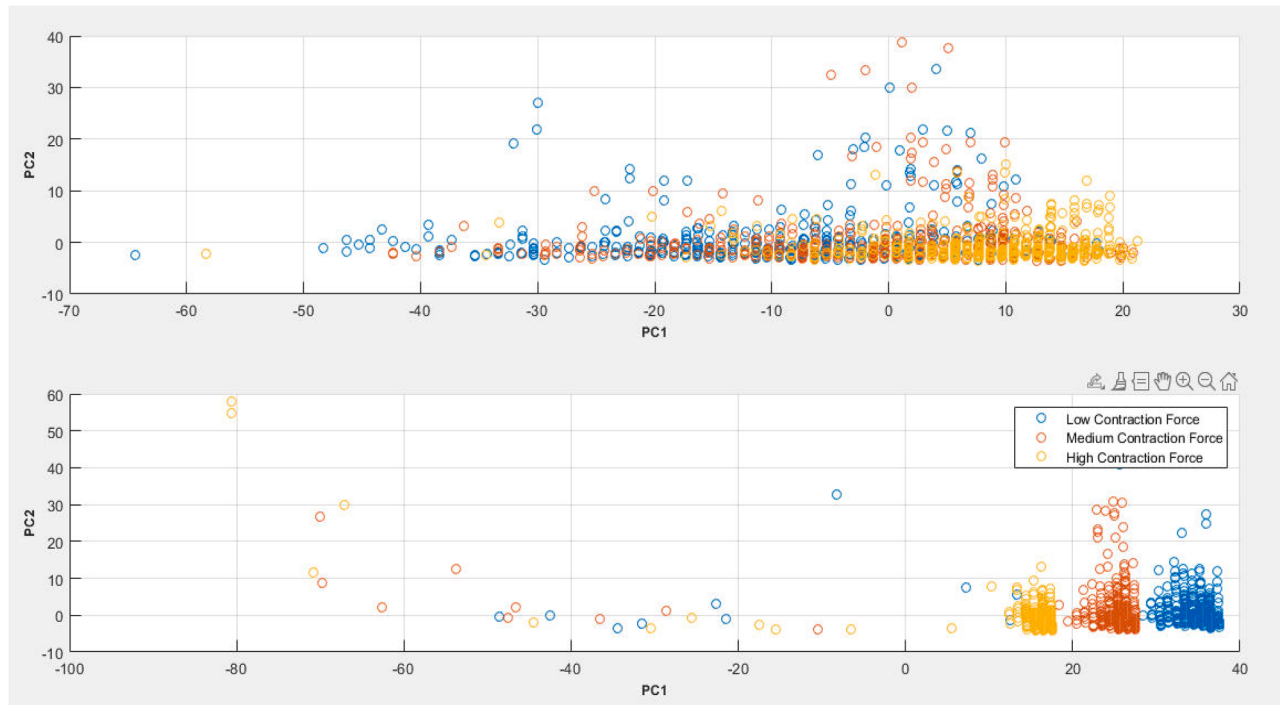


**Fig. 4.** PCA plot with 98% variability for Gesture 2 of the Raw Data (Top) and LSDL (Bottom).

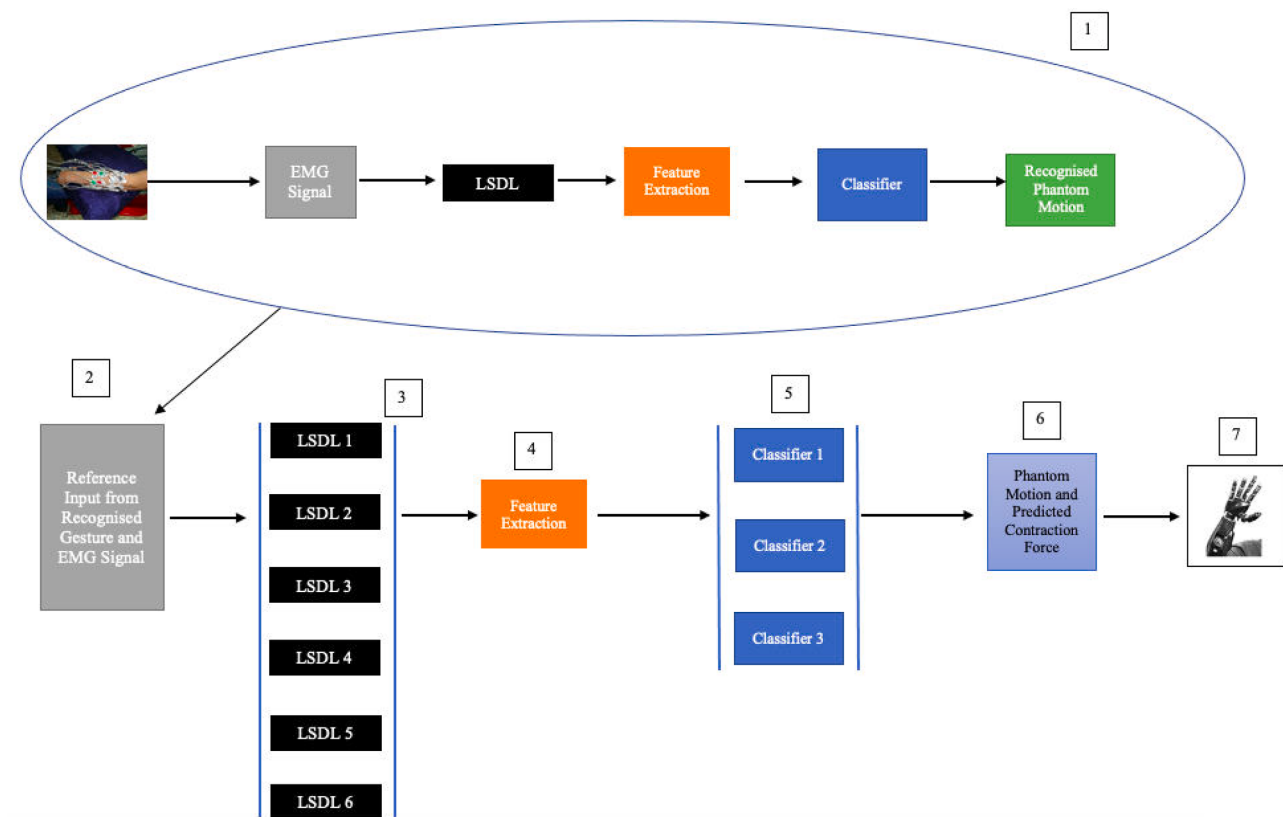


**Fig. 5.** Diagram showing both parts of the advanced pattern recognition control system, where the top part is the gesture recognition aspect addressed in previous work, and the bottom part involves the prediction of the contraction force.

## Data availability

Data will be made available on request.

## Acknowledgement

The author would like to thank Brian Kerr from Kerr Editing for proofreading this manuscript.

## Funding

This research was conducted as part of the work done at Nsugbe Research Labs

## Data availability

The data is available from a repository cited within the article.

## References

- Abdel-Basset, M., Abdel-Fatah, L., & Sangaiah, A. K. (2018). Chapter 10 - metaheuristic algorithms: A comprehensive review. In A. K. Sangaiah, M. Sheng, & Z. Zhang (Eds.), *Computational intelligence for multimedia big data on the cloud with engineering applications* (pp. 185–231). Academic Press. <https://doi.org/10.1016/B978-0-12-813314-9.00010-4>.
- Al-Timemy, A., Khushaba, R., Bugmann, G., & Escudero, J. (2015). Improving the performance against force variation of EMG controlled multifunctional upper-limb prostheses for transradial amputees. *IEEE Transactions on Neural Systems and Rehabilitation Engineering: A Publication of the IEEE Engineering in Medicine and Biology Society*. <https://doi.org/10.1109/TNSRE.2015.2445634>
- Analog.com. (n.d.). Analog control variable gain amplifiers (VGAs) | analog devices. Analog. Com. Retrieved 13 January 2022, from <https://www.analog.com/en/products/amplifiers/variable-gain-amplifiers/analog-control-vgas.html>.
- Attenberger, A., & Wojciechowski, S. (2017). A real-time classification system for upper limb prosthesis control in MATLAB. In R. Moreno-Díaz, F. Pichler, & A. Quesada-Arencibia (Eds.), *10672. Computer Aided Systems Theory – EUROCAST 2017: 16th International Conference, Las Palmas de Gran Canaria, Spain, February 19-24, 2017, Revised Selected Papers, Part II*. Springer International Publishing. <https://www.springerprofessional.de/en/a-real-time-classification-system-for-upper-limb-prosthesis-cont/15414932>.
- auto-sklearn. (n.d.). *auto-sklearn—AutoSklearn 0.14.7 documentation*. Automl.Github.Io. Retrieved 10 July 2022, from <https://automl.github.io/auto-sklearn/master/>.
- Barry, D., Leonard, J., Gitter, A., & Ball, R. D. (1986). Acoustic myography as a control signal for an externally powered prosthesis. *Archives of Physical Medicine and Rehabilitation*. <https://doi.org/10.5555/URI:PII:0003999386903941>
- Brownlee, J. (2020). TPOT for automated machine learning in python. *Machine Learning Mastery*. <https://machinelearningmastery.com/tpot-for-automated-machine-learning-in-python/>.
- Cao, F., Ye, H., & Wang, D. (2015). A probabilistic learning algorithm for robust modeling using neural networks with random weights. *Information Sciences*, 313, 62–78. <https://doi.org/10.1016/j.ins.2015.03.039>
- CompEngine. (n.d.). *CompEngine: a self-organizing database of time-series data*. Comp-Engine.Org. <https://www.comp-engine.org/>.
- Daubechies, I. (1992). *Ten lectures on wavelets*. Society for Industrial and Applied Mathematics.
- Doheny, E. P., Lowery, M. M., Fitzpatrick, D. P., & O’Malley, M. J. (2008). Effect of elbow joint angle on force-EMG relationships in human elbow flexor and extensor muscles. *Journal of Electromyography and Kinesiology: Official Journal of the International Society of Electrophysiological Kinesiology*, 18(5), 760–770. <https://doi.org/10.1016/j.jelekin.2007.03.006>
- Fougner, A., Stavdahl, O., Kyberd, P. J., Losier, Y. G., & Parker, P. A. (2012). Control of upper limb prostheses: Terminology and proportional myoelectric control—a review. *IEEE Transactions on Neural Systems and Rehabilitation Engineering: A Publication of the IEEE Engineering in Medicine and Biology Society*, 20(5), 663–677. <https://doi.org/10.1109/TNSRE.2012.2196711>
- Guo, W., Sheng, X., Liu, H., & Zhu, X. (2015). Development of a multi-channel compact-size wireless hybrid sEMG/NIRS sensor system for prosthetic manipulation. *IEEE Sensors Journal*, 16. <https://doi.org/10.1109/JSEN.2015.2459067>, 1–1.
- Guo, W., Sheng, X., Liu, H., & Zhu, X. (2017a). Mechanomyography assisted myoelectric sensing for upper-extremity prostheses: A hybrid approach. *IEEE Sensors Journal*. <https://doi.org/10.1109/JSEN.2017.2679806>
- Guo, W., Sheng, X., Liu, H., & Zhu, X. (2017b). Toward an enhanced human-machine interface for upper-limb prosthesis control with combined EMG and NIRS signals. *IEEE Transactions on Human-Machine Systems*, 47(4), 564–575. <https://doi.org/10.1109/THMS.2016.2641389>
- Guo, W., Yao, P., Sheng, X., Zhang, D., & Zhu, X. (2014). An enhanced human-computer interface based on simultaneous sEMG and NIRS for prostheses control. In *2014 IEEE International Conference on Information and Automation (ICIA)* (pp. 204–207). <https://doi.org/10.1109/ICInFA.2014.6932653>
- Limbless Statistics. (n.d.). *LIMBLESS statistics*. Limbless Statistics. Retrieved 27 December 2021, from <http://www.limbless-statistics.org/>.
- Lubba, C. H., Sethi, S. S., Knaute, P., Schultz, S. R., Fulcher, B. D., & Jones, N. S. (2019). catch22: CAnonical time-series characteristics. *Data Mining and Knowledge Discovery*, 33(6), 1821–1852. <https://doi.org/10.1007/s10618-019-00647-x>
- Nazarpour, K., Al-Timemy, A. H., Bugmann, G., & Jackson, A. (2013). A note on the probability distribution function of the surface electromyogram signal. *Brain Research Bulletin*, 90, 88–91. <https://doi.org/10.1016/j.brainresbull.2012.09.012>
- Nsugbe, E. (Unpublished results). *On the Gesture Recognition of a Faint Phantom Motion for the Control of a Transradial Prosthesis amidst varying Contraction Forces*.
- Nsugbe, E. (2017). *Particle size distribution estimation of a powder agglomeration process using acoustic emissions* [Thesis]. <http://dspace.lib.cranfield.ac.uk/handle/1826/14378>.
- Nsugbe, E. (2021a). Brain-machine and muscle-machine bio-sensing methods for gesture intent acquisition in upper-limb prosthesis control: A review. *Journal of Medical Engineering & Technology*, 45(2), 115–128. <https://doi.org/10.1080/03091902.2020.1854357>
- Nsugbe, E. (2021b). A pilot exploration on the use of NIR monitored haemodynamics in gesture recognition for transradial prosthesis control. *Intelligent Systems with Applications*, 9, Article 200045. <https://doi.org/10.1016/j.iswa.2021.200045>
- Nsugbe, E. (2021c). An insight into phantom sensation and the application of ultrasound imaging to the study of gesture motions for transhumeral prosthesis. *International Journal of Biomedical Engineering and Technology*.
- Nsugbe, E., & Al-Timemy, A. H. (2021). Shoulder girdle recognition using electrophysiological and low frequency anatomical contraction signals for prosthesis control. *CAAI Transactions on Intelligence Technology*, n/a(n/a). <https://doi.org/10.1049/cit2.12058>
- Nsugbe, E., Al-Timemy, A.H., . & Samuel, O.W. (Unpublished results). *Intelligence combiner: A combination of deep learning and handcrafted features for an adolescent psychosis prediction using EEG signals*.
- Nsugbe, E., Phillips, C., Fraser, M., & McIntosh, J. (2020a). Gesture recognition for transhumeral prosthesis control using EMG and NIR. *IET Cyber-Systems and Robotics*, 2(3), 122–131. <https://doi.org/10.1049/iet-csr.2020.0008>
- Nsugbe, E., Ruiz-Carcel, C., Starr, A., & Jennions, I. (2018). Estimation of fine and oversize particle ratio in a heterogeneous compound with acoustic emissions. *Sensors*, 18(3), 851. <https://doi.org/10.3390/s18030851>
- Nsugbe, E., Samuel, O. W., Asogbon, M. G., & Li, G. (2020b). A self-learning and adaptive control scheme for phantom prosthesis control using combined neuromuscular and brain-wave bio-signals. *Engineering Proceedings*, 2(1), 59. <https://doi.org/10.3390/ecsa-7-08169>
- Nsugbe, E., Samuel, O. W., Asogbon, M. G., & Li, G. (2021). Phantom motion intent decoding for transhumeral prosthesis control with fused neuromuscular and brain wave signals. *IET Cyber-Systems and Robotics*, 3(1), 77–88. <https://doi.org/10.1049/csy2.12009>
- Nsugbe, E., & Sanusi, I. (2021). Towards an affordable magnetomyography instrumentation and low model complexity approach for labour immminency prediction using a novel multiresolution analysis. *Applied AI Letters*, 2(3). <https://doi.org/10.1002/ail.234>
- Nsugbe, E., Starr, A., Foote, P., Ruiz-Carcel, C., & Jennions, I. (2016). Size differentiation of a continuous stream of particles using acoustic emissions. *IOP Conference Series: Materials Science and Engineering*, 161, Article 012090. <https://doi.org/10.1088/1757-899X/161/1/012090>
- Nsugbe, E., Williams Samuel, O., Asogbon, M. G., & Li, G. (2021). Contrast of multi-resolution analysis approach to transhumeral phantom motion decoding. *CAAI Transactions on Intelligence Technology*, 6(3), 360–375. <https://doi.org/10.1049/cit2.12039>
- ottobockus.com. (n.d.). *Bebionic® the world's most lifelike bionic hand*. Ottobockus.Com. [https://www.ottobockus.com/media/local-media/prosthetics/upper-limb/files/14112\\_bebionic\\_user\\_guide.lo.pdf](https://www.ottobockus.com/media/local-media/prosthetics/upper-limb/files/14112_bebionic_user_guide.lo.pdf).
- Patel, D., Yousaf Shah, S., Zhou, N., Shrivastava, S., Iyengar, A., Bhamidipaty, A., et al. (2020). FLops: On learning important time series features for real-valued prediction. In *2020 IEEE International Conference on Big Data (Big Data)* (pp. 1624–1633). <https://doi.org/10.1109/BigData50022.2020.9378499>
- scikit-learn. (n.d.). *Scikit-learn: Machine learning in python—Scikit-learn 1.1 documentation*. Scikit-Learn.Org. Retrieved 10 July 2022, from <https://scikit-learn.org/stable/>.
- Sharma, H., & Kumar, S. (2016). *A survey on decision tree algorithms of classification in data mining*. *International Journal of Science and Research (IJSR)*, 5.
- Stallone, A., Ciccone, A., & Materassi, M. (2020). New insights and best practices for the successful use of Empirical Mode Decomposition, Iterative Filtering and derived algorithms. *Scientific Reports*, 10(1), 15161. <https://doi.org/10.1038/s41598-020-72193-2>
- Statsmodels.org. (n.d.). *statsmodels.tsa.seasonal.seasonal\_decompose—Statsmodels*. Statsmodels.Org. Retrieved 10 July 2022, from [https://www.statsmodels.org/dev/generated/statsmodels.tsa.seasonal.seasonal\\_decompose.html](https://www.statsmodels.org/dev/generated/statsmodels.tsa.seasonal.seasonal_decompose.html).
- Talebi, S. (2022). *The wavelet transform*. May 24. Medium <https://towardsdatascience.com/the-wavelet-transform-e9cfa85d7b34>.
- Too, J., Abdullah, A. R., & Saad, N. M. (2019). Classification of hand movements based on discrete wavelet transform and enhanced feature extraction. *International Journal of Advanced Computer Science and Applications (IJACSA)*, 10(6). <https://doi.org/10.14569/IJACSA.2019.0100612>. Article 6.